

Fractional plateaus of the Coulomb blockade of coupled quantum dots

Karyn Le Hur

Département de Physique and CERPEMA, Université de Sherbrooke, Québec, Canada J1K 2R1.

Ground-state properties of a double-large-dot sample connected to a reservoir via a single-mode point contact are investigated. When the interdot transmission is *perfect* and the dots controlled by the same dimensionless gate voltage, we find that for any finite backscattering from the barrier between the lead and the left dot, the average dot charge exhibits a Coulomb-staircase behavior with steps of size $e/2$ and the capacitance peak period is halved. The interdot electrostatic coupling here is weak. For strong tunneling between the left dot and the lead, we report a conspicuous intermediate phase in which the fractional plateaus get substantially altered by an increasing slope.

PACS numbers: 73.23.Hk, 72.15.Qm, 73.40.Gk

I. INTRODUCTION

At low temperature, the charge on an isolated metallic grain (micronmetric dot) is known to be quantized in units of the electron charge e . Even when the grain is weakly-coupled to a bulk lead, so that electrons can occasionally hop from the lead to the dot and back, the grain charge remains to a large extent quantized¹. This is commonly referred to as the Coulomb blockade². In the opposite limit of perfect transmission between the reservoir and the dot, the average dot charge now depends (in a continuous manner) linearly on the applied gate voltage and the Coulomb blockade disappears³. However, Matveev has shown that a crossover from the linear charge-voltage dependence to a *Coulomb-staircase* function occurs for any finite backscattering from the quantum point contact (QPC) between the grain and the lead⁴. The physics remains qualitatively unchanged by increasing the reflection amplitude at the QPC.

Furthermore, close to the steps, the charge exhibits a nonanalytic logarithmic dependence on the voltage due to the presence of *two* spin channels entering the dot, resulting in an underlying two-channel Kondo model⁵.

Note also that the Coulomb blockade can be smeared out by applying an in-plane magnetic field⁶.

A direct measurement of the average grain charge, has been made possible using a single-electron transistor (SET) which has a sensitivity well below a single charge as well as a small input capacitance^{2,7}. In particular, some of the predictions above have been checked experimentally and its superiority to conductance measurements of charge fluctuations demonstrated⁸.

Here, we investigate exotic Coulomb staircases with fractional plateaus.

The simplest system we consider comprises two *large* symmetric dots, which can be viewed as an artificial molecule, connected to a single reservoir via a single-mode QPC (Fig. 1). For a recent review on artificial molecules built up with two dots, see Ref. 9. Here, each dot is coupled with the same capacitance C_{gd} to a side-gate. The term “large dot” implies that the spacing $\Delta \sim L^{-2}$ of the energy levels on each dot vanishes compared to the dot’s charging energy $E_c = e^2/(2C_\Sigma) \sim L^{-1}$

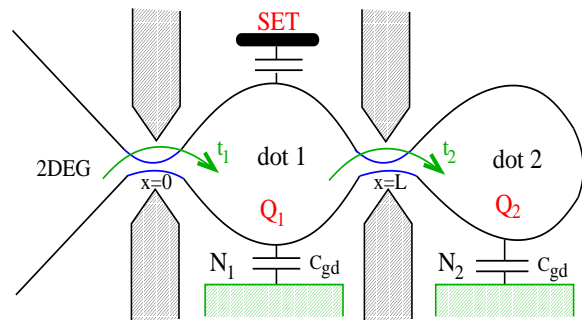


FIG. 1: A two-dimensional electron gas (2DEG) is coupled to two *large* dots via a single-mode QPC. The number of electrons Q_i on each dot is controlled via the dimensionless gate voltage N_i ; The case of interest here is $N_1 = N_2 = N$. The auxiliary gates can be used to adjust the conductances at the QPCs. A SET may probe the average charge on a single dot.

where $C_\Sigma \approx C_{gd}$. We already stress that strong tunneling between the dots (“covalent binding”) is required in order to find Coulomb staircases with fractional steps.

For example, when the interdot transmission is *perfect* and dot 1 is *weakly*-coupled to the lead, the interdot charge fluctuations are so strong that only the total charge of the two dots, $eQ = e(Q_1 + Q_2)$, can be *quantized* (but not the charge eQ_i on an individual dot). Thus, the electrostatic Hamiltonian of the two dots can be rewritten more conveniently as (for details, see Refs. 10,11)

$$H_c[N] = \frac{E_c}{2}(Q - 2N)^2 + 2E_c\left(Q_1 - \frac{Q}{2}\right)^2 - 2E_cN^2. \quad (1)$$

The interdot capacitive coupling is *weak* in order to maximize the interdot charge fluctuations¹². Moreover, the symmetric dots are controlled by the same gate voltage V_G and $N = V_G C_{gd}/e$. From the electrostatic Hamiltonian, it can be easily inferred that the double dot behaves as a single **composite conductor** of quantized charge $eQ = 2e\bar{Q}_1$ determined by the total gate voltage $2N$. When an electron tunnels into the left dot, i.e., $Q = 1$, this implies that a charge e is fluctuating back and forth between the dots and clearly $\bar{Q}_{i=1,2}[N]$ exhibits steps of size $1/2$ ¹³. Moreover, close to a point $2N^* = (2n + 1)/2$ ($n \in \mathcal{N}$), the charge states with $Q = n$ ($\bar{Q}_1 = n/2$)

and $Q = n + 1$ ($\bar{Q}_1 = n/2 + 1/2$) are degenerate resulting in (sharp) peaks in the single dot capacitance $C_1 \propto \partial \bar{Q}_1 / \partial N$ (Fig. 2). Similar to the *conductance* peaks for two large dots tunnel-coupled to leads^{10,11}, we then observe that strong interdot charge fluctuations produce the *halving* of the capacitance peak period. For an experimental proof, see e.g. Ref. 14

Based on two-impurity two-channel Kondo models (2CKMs) (small dots coupled to leads are described by a two-impurity 1CKM¹⁵), below we thoroughly analyze the evolution of the fractional steps as a function of the hopping parameters t_1 and t_2 (Fig. 1). Some aspects of the problem will join up with previous works on the conductance through a double (large) dot structure^{10,11}.

From here on, we assume that a single orbital channel with two spin polarizations $\alpha = \uparrow, \downarrow$ enters the double dot. Again, we assume that the level spacing on each dot (almost) vanishes which means that we consider a *continuous* spectrum in each dot and we neglect the mesoscopic corrections to the capacitance C_{gd} ; the size of a dot can thus exceed the effective Bohr radius ($\sim \mu m$ in Refs. 8,14). Temperature will be taken to be zero ($T = 0$).

II. WEAK COUPLING WITH LEAD

Weak tunneling ($t_1 \ll 1$) between the lead and the composite dot produces corrections to the Coulomb staircase behavior found above.

More precisely, for perfect interdot transmission ($t_2 \rightarrow 1$), we can describe the *composite dot* in the vicinity of the two QPCs by the same field operator $\Psi_{c\alpha}(x)$. Additionally, close to a degeneracy point $N^* = (2n + 1)/4$, only the states with $Q = n$ and $Q = n + 1$ are allowed and, thus, following Ref. 1, the tunneling Hamiltonian for this truncated system takes the form:

$$H_t = \sum_{\alpha} \left(t_1 \Psi_{c\alpha}^{\dagger}(0) \Psi_{r\alpha}(0) S^+ + h.c. \right). \quad (2)$$

$\Psi_{r\alpha}$ stands for the electron operator in the *lead*, and the spin operator S^+ guarantees that when an electron tunnels into the *double dot*, the total charge Q only changes from n to $n + 1$ ^{1,6}; we then have the equalities¹⁶

$$\bar{Q} = 2\bar{Q}_1 = (n + 1/2) + \bar{S}_z. \quad (3)$$

Following the route of the single-dot problem^{1,6}, now we can identify $s_{\alpha}^{-}(0) = \Psi_{c\alpha}^{\dagger}(0) \Psi_{r\alpha}(0)$ as an electron pseudo-spin operator acting on the (orbital) indices $j = r, c$ and finally recover a 2CKM^{5,17}. The two channels are the two spin states of an electron. In particular, Eq. (1) can be viewed as a local magnetic field $\hbar S_z$ with $\hbar \propto (2n + 1 - 4N)$. This results in

$$\bar{Q}_1 - \frac{2n + 1}{4} \propto (2n + 1 - 4N) \ln \left(\left| N - \frac{2n + 1}{4} \right| \right). \quad (4)$$

To sum it up, we recover a standard logarithmic form

$$\delta C_1 = C_1 - C_{gd} \propto -\ln \left(\left| N - \frac{2n + 1}{4} \right| \right), \quad (5)$$

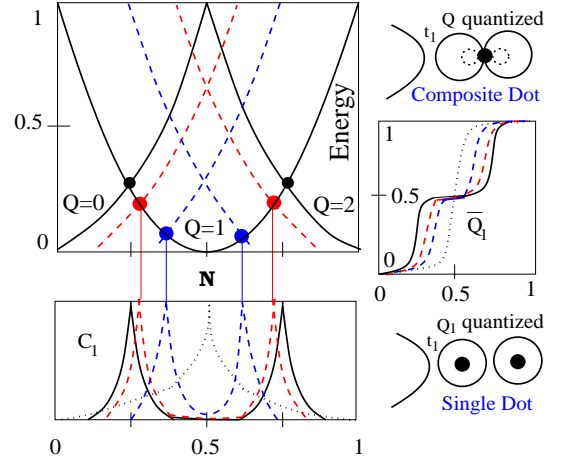


FIG. 2: Charging energies ($+\delta E$) of the “composite” dot as a function of N given in units of E_c ; t_1 is *small*. Each eigenstate with $Q = n$ gives rise to a parabola. The solid lines correspond to $r_2 = 0$ and dashed lines to increasing r_2 couplings. For $r_1 = 1 - t_1 \rightarrow 1$, Q is quantized and for symmetric dots this guarantees $\bar{Q}_1 = n/2$ until $r_2 \rightarrow 1$ (Eqs. (11),(24)).

for the capacitance peaks.

We now discuss the situation in which the interdot tunneling is strongly decreased, ($t_1; t_2$) $\ll 1$. Each dot is described by its own operator $\Psi_{i\alpha}$ and the Coulomb term should be written in a more common way as^{11,12}:

$$H_c^1[N] + H_c^2[N] = E_c \sum_{i=1,2} (Q_i - N)^2 - 2E_c N^2. \quad (6)$$

When $t_2 \rightarrow 0$, we converge to a **single-dot** problem^{1,6}: Q_1 is quantized and we could not use $\bar{Q}_1 \sim Q/2$ in Eq.(1)! The degeneracy points now occur for $N_s^* = (2k + 1)/2$ ($k \in \mathcal{N}$) and obviously the period of the capacitance peaks then *doubles* (Fig. 2).

As soon as t_2 is finite ($t_2 \sim t_1$) and $N \approx 1/2$, we propose to modify the tunneling Hamiltonian as:

$$H_t = \sum_{\alpha} \left(t_1 \Psi_{1\alpha}^{\dagger}(0) \Psi_{r\alpha}(0) + t_2 \Psi_{2\alpha}^{\dagger}(L) \Psi_{1\alpha}(L) + h.c. \right) \quad (7)$$

$$= \sum_{\alpha} \left(t_1 s_{\alpha}^{-}(0) S_1^+ + t_2 s_{\alpha}^{-}(L) S_2^+ + h.c. \right),$$

where $S_1^+(S_2^+)$ emphasizes that the charge on dot 1(2) only changes from 0 to 1; For more details, see note 18.

Again, the index $j = 1, 2, r$ -which designates the location of an electron in the setup- in the $\Psi_{j\alpha}$ operator can mimic an internal “orbital” degree of freedom. It is then straightforward to define two spin operators at $x = (0, L)$ acting on the orbital space, similar as in Ref. 1:

$$s_{\alpha}^{-}(0) = \Psi_{1\alpha}^{\dagger}(0) \Psi_{r\alpha}(0) \quad (8)$$

$$s_{\alpha}^{-}(L) = \Psi_{2\alpha}^{\dagger}(L) \Psi_{1\alpha}(L).$$

This two-impurity (two-channel) Kondo model is particularly convenient to revisit the behavior of charge fluctuations close to the degeneracy points N_s^* ; the crucial

point being that a finite bare coupling t_2 (like t_1) will be strongly renormalized at low temperatures¹⁹.

At the fixed point ($T = 0$) and, e.g., close to the *degeneracy* point $N_s^* = 1/2$, the two dots will *merge* into one and therefore by analogy to Eq. (3) we must correctly reidentify

$$\bar{Q} = (j + 1/2) + \bar{S}_z = 2\bar{Q}_1, \quad (9)$$

where $j = (0; 1)$ ²⁰. Moreover, the Coulomb term in the fixed-point basis takes the form hS_z where $h \propto (1 - 2N \mp 2\kappa\mathcal{T}_2)$ for $j = (0; 1)$; $\mathcal{T}_2 = (t_2)^2$ and $\kappa > 0$. Away from the point $N_s^* = 1/2$, second order perturbation theory in t_2 is accurate, and we have taken into account the relative energy shift between *even* and *odd* Q-states^{10,11}:

$$\delta E \propto -4\mathcal{T}_2 \ln 2. \quad (10)$$

Similar to Eq. (4), we are thus led to (for $j = 0, 1$ respectively)

$$\bar{Q}_1 = \begin{cases} \frac{1}{4} - b \left(N - \frac{1}{2} + \kappa\mathcal{T}_2 \right) \ln \left(\left| N - \frac{1}{2} + \kappa\mathcal{T}_2 \right| \right), \\ \frac{3}{4} - b \left(N - \frac{1}{2} - \kappa\mathcal{T}_2 \right) \ln \left(\left| N - \frac{1}{2} - \kappa\mathcal{T}_2 \right| \right). \end{cases} \quad (11)$$

$b > 0$ is a parameter which is inversely proportional to the Kondo energy scale. By continuity, a tiny step appears at $\bar{Q}_1 = 1/2$, and the single-dot capacitance peaks are already split by $\sim 2\kappa\mathcal{T}_2$ (Fig. 2).

The progressive pairing of the capacitance sub-peaks close to $t_2 = 1$ will be studied later (Eq. (24)).

III. STRONG COUPLING WITH LEAD

Now, we mainly consider the case where all the junctions have conductances close to $2e^2/h$, i.e., reflection amplitudes are small ($r_1; r_2 \ll 1$).

In this case, the whole system can be viewed as a single conductor and, for convenience, we will use the unique field operator $\Psi_{r\alpha}(x)$ ²¹. We can write $\Psi_{r\alpha}(x) = \exp(ik_F x) \Psi_{+\alpha}(x) + \exp(-ik_F x) \Psi_{-\alpha}(x)$, $\Psi_{+\alpha}$ and $\Psi_{-\alpha}$ describe right- and left-moving fermions respectively. The kinetic energy obeys

$$H_k = iv_F \int_{-\infty}^{+2L} dx \left(\Psi_{+\alpha}^\dagger \partial_x \Psi_{+\alpha} - \Psi_{-\alpha}^\dagger \partial_x \Psi_{-\alpha} \right), \quad (12)$$

v_F being the Fermi velocity. The backscattering term(s) takes the standard form:

$$H_b = v_F \sum_{\alpha} \left(r_{1,2} \Psi_{+\alpha}^\dagger(0, L) \Psi_{-\alpha}(0, L) + h.c. \right), \quad (13)$$

and interactions in a grain are embodied via the general Coulomb Hamiltonians $H_c[N_1] + H_c[N_2]$, in Eq. (6).

At low energy, we proceed with this model by bosonization of the one-dimensional Fermi fields⁶. In those variables, the kinetic energy yields a separation of the spin

and charge and the resulting Hamiltonians have plasmon-like excitations. Here, $\partial_x \phi_j$ with $j = (c, s)$ measures fluctuations of charge/spin density and $\Pi_j = \partial_x \theta_j$ being its conjugate momentum. The Coulomb Hamiltonians take the forms (We could also employ Eq. (1)):

$$H_c^1[N_1] = \frac{2E_c}{\pi} \left(\phi_c(0) - \phi_c(L) - \sqrt{\frac{\pi}{2}} N_1 \right)^2 - E_c N_1^2 \quad (14)$$

$$H_c^2[N_2] = \frac{2E_c}{\pi} \left(\phi_c(L) - \phi_c(2L) - \sqrt{\frac{\pi}{2}} N_2 \right)^2 - E_c N_2^2.$$

To minimize the Coulomb energies when the transmissions at the two QPCs are *both* perfect, we easily recover that the dot's charges evolve continuously (linearly) as a function of the gate voltages^{3,4}:

$$\bar{Q}_1 = \frac{\sqrt{2}}{\pi} (\phi_c(0) - \phi_c(L)) = N_1 \quad (15)$$

$$\bar{Q}_2 = \frac{\sqrt{2}}{\pi} (\phi_c(L) - \phi_c(2L)) = N_2.$$

Remember that for $r_1 = r_2 = 0$, the Coulomb blockade physics is totally suppressed. In our geometry there are no charge fluctuations at $x = 2L$ and then $\phi_c(2L) = cst$.

Furthermore, following the traditional route of the single-dot problem for this regime^{4,6}, the backscattering term may be rewritten as

$$H_b = \frac{\sqrt{\gamma a E_c v_F}}{\pi a} 4r_1 \cos(\pi(N_1 + N_2)) \cos\left(\sqrt{2\pi} \phi_s(0)\right) \mathcal{T}_{1x} \quad (16)$$

$$+ \frac{\sqrt{\gamma a E_c v_F}}{\pi a} 4r_2 \cos(\pi N_2) \cos\left(\sqrt{2\pi} \phi_s(L)\right) \mathcal{T}_{2x}.$$

Since the charge fluctuations on each dot cannot depend on the precise size of a dot, we must equate $\phi_c(2L) = 2k_F L / \sqrt{2\pi}$ and rescale $\phi_c(0) \rightarrow \phi_c(0) + 2k_F L / \sqrt{2\pi}$. Here γ obeys $\gamma = e^{\mathcal{C}}$ where $\mathcal{C} \approx 0.5772...$ is the Euler-Mascheroni constant and a is a short-distance cutoff. We have introduced two *commuting* impurity spins \mathcal{T}_1 and \mathcal{T}_2 (which here are **not** related to the charge on each dot). Clearly, the \mathcal{T}_{1x} and \mathcal{T}_{2x} spin-operators both commute with the Hamiltonian and must be simply identified as c-numbers, i.e., $\mathcal{T}_{1x} = 1/2$ (or $-1/2$) and similarly for \mathcal{T}_{2x} . Eq. (16) must be viewed as an extension of the 2CKM at the Emery-Kivelson limit²².

To compute the correction to the average dot charge(s), here we must “de-bosonize” the problem as^{4,6}

$$H_b \approx \frac{iJ_{1x}}{\sqrt{4\pi a}} (\psi(0) + \psi^\dagger(0)) \zeta_1 \quad (17)$$

$$+ \frac{iJ_{2x}}{\sqrt{4\pi a}} (\psi(L) + \psi^\dagger(L)) \zeta_2.$$

ζ_1 and ζ_2 are two Majorana fermions, and the Kondo exchanges above read $J_{1x} = 4r_1 \sqrt{a\gamma E_c v_F} \cos(\pi(N_1 + N_2))$ and $J_{2x} = 4r_2 \sqrt{a\gamma E_c v_F} \cos(\pi N_2)$. In the absence of an applied magnetic field, there is no net magnetization and no spin current on the whole region $[-L; L]$ and, thus, we have approximated²¹ $\psi(L) \approx \exp(i\sqrt{2\pi} \phi_s(L))$ (For more

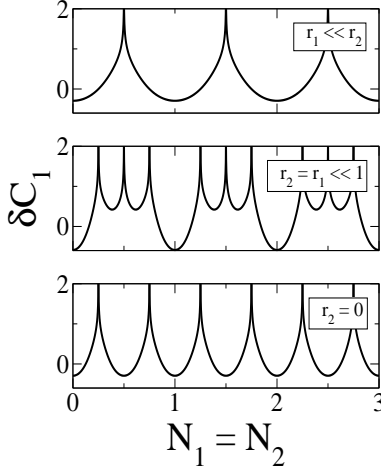


FIG. 3: Dot's differential capacitance for *small* $r_1 = 0.4$. For $r_2 \approx 0$ the system behaves as a *single composite conductor* whereas for $r_2 \rightarrow 1$ we must recover a *single-dot* problem. For $r_2 \approx r_1 \ll 1$ the system cannot decide between those two ground states giving a “3-peak” capacitance profile, i.e., unstable fractional steps (Fig. 4 and Eq. (22)): Charge fluctuations are important at $N = 1/4$ and at $N = 1/2$ as well.

explanation, see Ref. 6). The fermionic model here generates two Kondo resonances

$$\Gamma_1 = \frac{J_{1x}^2}{4\pi av_F} = \frac{E_c \gamma}{\pi} (2r_1)^2 \cos^2(\pi(N_1 + N_2)) \quad (18)$$

$$\Gamma_2 = \frac{J_{2x}^2}{4\pi av_F} = \frac{E_c \gamma}{\pi} (2r_2)^2 \cos^2(\pi N_2),$$

and all the quantities of interest will be now inferred from the quantum correction of the ground state energy

$$\delta E = -\frac{\Gamma_1}{\pi} \ln(E_c/\Gamma_1) - \frac{\Gamma_2}{\pi} \ln(E_c/\Gamma_2), \quad (19)$$

which implies that impurities are *independently* screened. Let us discuss the case of symmetric dots: $N_1 = N_2 = N$. The correction to the average charge on each dot $\delta \bar{Q}_i$ and the dot's differential capacitance δC_i obey: $\delta \bar{Q}_i = \bar{Q}_i - N \propto -\partial \delta E / (E_c \partial N)$ and $\delta C_i \propto \partial \delta \bar{Q}_i / \partial N$. For clarity's sake, results have been summarized in Figs. 3,4.

A. $r_2 \rightarrow 0$

For a double dot connected by a reflectionless constriction $0 \leftarrow r_2 \ll r_1 (\ll 1)$, using the formulas above, we easily recover fractional charge plateaus with steps $1/2$ and capacitance peaks with halved period. Again, the double dot behaves as a **single composite conductor** of *quantized* charge $Q \approx 2\bar{Q}_1$. In particular, we predict that the logarithmic singularity $\delta C_i \propto -\ln(|N - \frac{1}{4}|)$ should be observed at any value of $t_1 \neq 1$ (as nicely illustrated in Figs. 3 and 4).

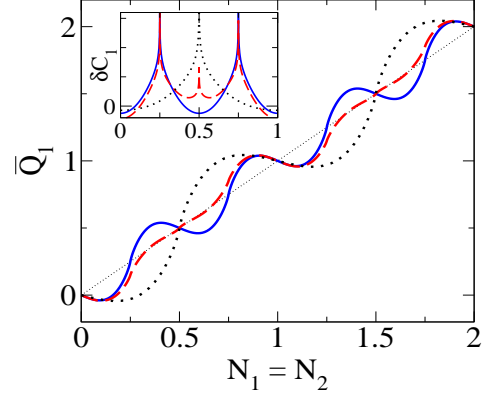


FIG. 4: Evolution of the fractional plateaus for *small* r_1 . (Note e.g. that for $r_2 = 0$ we have only taken into account the main leading term when taking the derivate of Eq. (19), which explains the “slightly” negative slope in the middle of a plateau). The solid line is for $r_1 = 0.2$ and $r_2 = 0$, the dashed line for $r_1 = r_2 = 0.15$ (fractional plateaus now acquire a *positive* slope) and the dotted line for $r_1 = 0.3$ and $r_2 \rightarrow 1$.

B. $r_2 \rightarrow 1$

In the opposite limit $r_1 \ll r_2 \rightarrow 1$, the interdot constriction considerably impedes the charge spreading between the dots. Q_2 becomes an integer-valued operator describing electrons which tunnel into the dot 2 (Eq.(6)) and charge fluctuations in dot 1 closely resemble the ones of a **single dot** which is strongly-coupled to one lead:

$$H_b \propto r_1 (-1)^{Q_2} \cos(\pi N) \cos\left(\sqrt{2\pi} \phi_s(0)\right) \mathcal{T}_{1x}. \quad (20)$$

The Kondo energy scale

$$\Gamma_1 = \frac{E_c \gamma}{\pi} (2r_1)^2 \cos^2(\pi N), \quad (21)$$

is identical to the one of the single-dot problem⁴, and assuming $r_1 \neq 0$, Q_1 becomes also *quantized*.

The small term $t_2 \Psi_{2\alpha}^\dagger(L) \Psi_{1\alpha}(L) S_2^+ + h.c.$ here mostly produces slight charge fluctuations in the dot 2, and $\delta C_2 \propto -\ln(|N - 1/2|)$.

C. $r_1 \approx r_2 \ll 1$

For $r_1 \approx r_2$, a strong opposition between the single-dot (Q_i is quantized for $r_2 \gg r_1$) and the composite-dot ground-state ($\bar{Q}_i = Q/2$ for $r_1 \gg r_2$) arises giving a fascinating “hybrid” regime where the fractional plateaus become gradually destroyed by acquiring a *positive* slope (Fig. 4); Close to $N = 1/2$, exploiting Eqs. (18) and (19), we can approximate $(f(\mathcal{R}_1) = \ln \mathcal{R}_1 + \text{const.})$

$$\delta \bar{Q}_1 \propto (N - 1/2) (\mathcal{R}_1 f(\mathcal{R}_1) - \mathcal{R}_2 \ln(|N - 1/2|)), \quad (22)$$

then inducing an exotic “3-peak” capacitance profile; $\mathcal{R}_i = (r_i)^2$ (inset in Fig. 4). The central peak becomes more pronounced by slightly increasing r_2 , whereas the external peaks only depends on r_1 (as long as $r_2 \ll 1$).

D. $r_1 \rightarrow 1$ and $r_2 \ll 1$

It is worthwhile to compare with the case $r_1 \rightarrow 1$ and $r_2 \ll 1$. Here, $Q = \sqrt{2/\pi}\phi_c(0) = n$ must be an *integer-valued* operator which guarantees $\bar{Q}_1 = n/2$. The fractional plateaus remain by decreasing the interdot coupling and only their widths progressively reduce: $N^*(n=1) - N^*(n=0) = 1/2 - 2\eta\mathcal{R}_2 \ln(1/\mathcal{R}_2)$; $\eta > 0$ is a constant parameter. More precisely, for $N_1 = N_2 = N$, it is easy to rewrite the backscattering term as:

$$H_b = \frac{\sqrt{\gamma a E_c v_F}}{\pi a} 4r_2 \cos\left(\frac{n\pi}{2}\right) \cos\left(\sqrt{2\pi}\phi_s(L)\right) \mathcal{T}_{2x}, \quad (23)$$

to Eqs. (1),(2) which then produces a Kondo energy scale $\Gamma_2 = E_c \gamma (2r_2)^2 \cos^2\left(\frac{n\pi}{2}\right)/\pi$, and then a relative energy shift $\delta E \propto \mathcal{R}_2 \ln(1/\mathcal{R}_2)$ between *even* and *odd* states^{10,11}. This engenders that the positions of the capacitance (sub-)peaks (furnished by Eq. 1) are shifted as

$$N^* = (2n+1)/4 + (-1)^n \eta \mathcal{R}_2 \ln(1/\mathcal{R}_2). \quad (24)$$

The capacitance (sub-)peaks are not equally spaced anymore and progressively pair around the points $N_s^* = (2n+1)/2$ (Fig. 2). Finally, we have checked that integer plateaus become more prominent: $N^*(n=2) - N^*(n=1) = 1/2 + 2\eta\mathcal{R}_2 \ln(1/\mathcal{R}_2)$.

IV. CONCLUSION

In closing, based on two-impurity two-channel Kondo models, we have presented a detailed discussion on the

evolution of the fractional plateaus as a function of the hopping parameters t_1 and t_2 for a double-dot coupled via a single-mode QPC to a reservoir.

Again, for *perfect* interdot transmission, Coulomb steps of size $1/2$ occur for any finite backscattering between the lead and the left dot. When an electron enters the artificial molecule, a charge 1 is fluctuating back and forth between the two dots. We are hopeful that this can be observed via capacitance measurements^{12,13}.

Substantially decreasing the interdot coupling inevitably restores the single-dot Coulomb blockade and the capacitance peak period *doubles*.

For strong coupling between the lead and the left dot ($r_1 \ll 1$), we find a striking intermediate range ($r_2 \approx r_1$) where the fractional steps become progressively unstable, i.e., show an increasing positive slope; this happens due to the strong competition between a *single-dot* and a *composite-dot* ground state. On the contrary, when $r_1 \rightarrow 1$, Q must be quantized and $\bar{Q}_1 = Q/2$; the fractional steps persist.

For *asymmetric* dots, e.g., with different gate-dot capacitances, we report that the Coulomb staircase with halved steps is gradually altered.

Acknowledgments: This work was supported by the Swiss National Science Foundation and is currently supported by NSERC. The author is grateful to R. C. Ashoori and K. A. Matveev for their comments.

-
- ¹ K. A. Matveev, Sov. Phys. JETP **72**, 892, (1991).
² *Single Charge Tunneling*, edited by H. Grabert and M. H. Devoret (Plenum Press, New York, 1992).
³ N. C. van der Vaart, A. T. Johnson, L. P. Kouwenhoven, D. J. Maas, W. de Jong, M. P. de Ruyter van Steveninck, A. van der Enden, C. J. P. M. Harmans, and C. T. Foxon, Phys. B **189**, 99 (1993); Yu. V. Nazarov, Phys. Rev. Lett. **82**, 1245 (1999).
⁴ K. A. Matveev, Phys. Rev. B **51**, 1743 (1995).
⁵ Ph. Nozières et al. Blandin, J. Phys. (Paris) **41**, 193 (1980).
⁶ K. Le Hur, Phys. Rev. B **64**, 161302(R) (2001); K. Le Hur and G. Seelig, Phys. Rev. B **65**, 165338 (2002).
⁷ P. Lafarge, P. Joyez, D. Esteve, C. Urbina, and M. H. Devoret, Nature (London) **365**, 422 (1993).
⁸ D. Berman, N. B. Zhitenev, R. C. Ashoori, and M. Shayegan, Phys. Rev. Lett. **82**, 161 (1999); D. S. Duncan, C. Livermore, and R. M. Westervelt, Applied Phys. Lett. **74**, 1045 (1999).
⁹ W. G. van der Wiel, S. De Franceschi, J. M. Elzerman, T. Fujisawa, S. Tarucha, and L. P. Kouwenhoven, Rev. Mod. Phys. Vol. 75 No. 1, 1-22 (2003).
¹⁰ K. A. Matveev, L. I. Glazman, and H. U. Baranger, Phys. Rev. B **53**, 1034 (1996); **54**, 5637 (1996).
¹¹ J. M. Golden and B. I. Halperin, Phys. Rev. B **53**, 3893 (1996); **65**, 115326 (2002) and references therein.
¹² An interdot capacitance C_m produces a (repulsive) term $Q_1 Q_2$ which would rather give $(Q_1, Q_2) = (1, 0)$ or $(0, 1)$: N. Andrei, G. T. Zimányi, and G. Schön, Phys. Rev. B **60**, 5125(R) (1999).
¹³ For $t_2 \rightarrow 1$, the typical time of those fluctuations is $t_c \sim \hbar/E_c$ (For $t_2 \ll 1$, t_c is much larger $\sim (\hbar/E_c)e^{1/t_2}$).
¹⁴ F. R. Waugh, M. J. Berry, D. J. Mar, R. M. Westervelt, K. L. Campman, and A. C. Gossard, Phys. Rev. Lett. **75**, 705 (1995).
¹⁵ A. Georges and Y. Meir, Phys. Rev. Lett. **82**, 3508 (1999).
¹⁶ For simplicity, charge is now normalized to e .
¹⁷ A. M. Tsvelik and P. B. Wiegmann, Z. Phys. B **54**, 201 (1984); N. Andrei and C. Destri, Phys. Rev. Lett. **52**, 364 (1984).
¹⁸ We may *equally* use $|\Phi >_i$ or $(|\Phi >_i * |Q_i >)$, where $|\Phi >_i$ is any state of the dot i with charge Q_i ; the (charge) state $|Q_i >$ must be viewed as an extra label to $|\Phi >_i$. When the tunneling process $t_2 \Psi_{2\alpha}^\dagger(L) \Psi_{1\alpha}(L)$ takes place, e.g., Q_2 changes from 0 to 1; this can be emphasized by the introduction of a pseudo-spin operator: $|Q_2 = 1 > = S_2^+ |Q_2 = 0 >^{1,6}$. This procedure gives another type of term (with

2 spin operators) $t_2 \Psi_{2\alpha}^\dagger(L) \Psi_{1\alpha}(L) S_2^+ S_1^-$; but, this is not “renormalized” at low energy and we ignore it. Again, here the coupling $S_{1z} S_{2z}$ ($Q_1 Q_2$) is negligible.

¹⁹ A. Georges and A. Sengupta, Phys. Rev. Lett. **74**, 2808 (1995).

²⁰ $Q \sim 2\bar{Q}_1$ takes the values 0,1 or 2 and $\Psi_{1\alpha} \rightarrow \Psi_{c\alpha}$.

²¹ We could also introduce two different wave functions for the two QPCs ($\psi(0) \rightarrow \psi_1(0)$, $\psi(L) \rightarrow \psi_2(0)$ in Eq.(17)).

²² V. J. Emery and S. Kivelson, Phys. Rev. B **46**, 10 812 (1992); A. M. Sengupta and A. Georges, *ibid.* **49**, 10 020 (1994).